Effect of Cu and Ni addition in Fe-Mn-Si shape memory alloy

S Balasubramani[1], Dr.T.Vigraman[2]

Abstract— The Fe-Mn-Si shape memory alloys (SMA) produced by powder metallurgy technique for various compositions with the addition of alloying elements nickel and copper were tested for it's tensile strength. A maximum tensile strength of 301 MPa was exhibited by the alloy having Fe-30%Mn-6%Si-1%Ni. It was compacted by applying a pressure of 560 MPa and sintered at a temperature of 1000 ℃. The SMA revealed a maximum hardness of 78 in Rockwell hardness 'B' scale. The effect of alloy additions on the microstructure and formation of various compounds of shape memory alloy were examined by Optical Microscopy. The shape memory effect and strain recovery of these alloys were studied by conducting bend test.

Index Terms— Alloy, powder metallurgy, shape memory effect, tensile test.

INTRODUCTION

SHAPE memory alloys can be classified into two broad categories one is ferrous alloys and another one is non-ferrous alloys. The ferrous SMA consists of 'Fe', 'Mn', alloys. But the shape memory effect exhibited by these alloys are one way, further, certain limitations are shown by these alloys on shape memory effect itself. Therefore, a need arises to investigate by adding alloying elements and varying the parameters to study the SMA effect. A shape memory alloy keeps the original shape in memory after deformation and regain it's original shape when it is heated. A shape memory material has unique characteristics of relationship between stress, strain and temperature and is based on crystallographic reversible thermoplastic martensitic transformation. The phase transformation taking place at low temperature is martensite and the transformation taking place at higher temperature is known as austenite as in steel.

The structure and shape memory effect of 60%Fe-29%Mn-11%Si alloy was studied by Karolina Gąska et al. The powders were mechanically alloyed for 30 hours in a planetary ball mill, compacted and sintered at 1027K. The investigations revealed γ-FCC and ε-HCP phases formed after mechanical alloying for 30 hours. These sample after mechanical alloying showed shape memory effect**.** Chenglao Li et al described the effect of Fe-Mn-Si-Cr-Ni shape memory alloy with the addition of alloying elements namely 'Ce', 'Ti' and 'N'. The shape memory effect was raised with the addition of 'Ce', on the other hand addition of 'Ti' and 'N' enhanced shape memory effect to a very high level. Nevin Balo et al studied the oxidation behavior of Fe–Mn–Si and Fe–Mn–Si–Cr SMA's under isothermal conditions. The oxidation of Fe-Mn-Si alloy was less with the addition of 'Cr' in Fe-Mn-Si alloy. The oxidation activation energies of the Fe–Mn–Si and Fe–Mn–Si–Cr alloys and 'Si' as major alloying elements and 'Ni' is added to these alloys to enhance corrosion resistant properties. The costs of the ferrous SMA's are less than non-ferrous were found to be 126.79kJ/mol and 105.74kJ/mol, respectively. The formed oxides for the Fe-Mn-Si and Fe-Mn-Si-Cr alloys were determined by XRD patterns. Shipu Chen et al investigated the effect of nitrogen on properties including shape memory effect, mechanical behavior and corrosion behavior of Fe–Mn–Si–Cr based alloys. The shape memory effect was improved with the addition of small amounts of nitrogen in Fe–25%Mn–6%Si–5%Cr alloys. The tested alloys containing more than 0.12 weight percentage of nitrogen showed an excellent shape memory effect. Nitrogen is an austenite stabilizing element; therefore, it strengthens the austenite phase by raising the critical stress to offset the slip planes and dislocations.

Kannan et al tested the corrosion resistant properties of the Fe–Mn–Al–Si alloy steel. The experiments were conducted in acidic (0.1 M H_2SO_4), alkaline (0.1 M NaOH) and chloride-containing (3.5% NaCl) environments, using immersion and polarization experiments, and compared with that of interstitial-free (IF) steel. In acidic solution, the Fe–Mn–Al–Si steel exhibited poor corrosion resistance which was attributed to the non-passivating tendency of aluminium in this medium and high-manganese dissolution in addition to iron dissolution in acidic medium. The Fe–Mn–Al–Si steel also showed higher corrosion resistance in alkaline solution than in acidic or in chloride-containing solutions. The higher corrosion resistance of the Fe–Mn–Al–Si steel in alkaline solution was mainly attributed to the passivating effect of manganese and iron. Pricop et al obtained SMA's by powder metallurgy technique and performed hot rolling to increase the density. In tensile, loading-unloading cycles the super elastic property was examined by increasing the number of mechanical cycles. The tensile specimens were cut after mechanical cycling and their structure was analyzed by XRD and SEM. SEM examinations revealed the presence of α'martensite. The increase in α'martensite was due to hot rolling**.**

- *S.Balasubramani is currently pursuing masters degree program in production engineering at National engineering college ,India, PH-9600786180. E-mail: balasubramanigs@gmail.com*
- *Dr.T.Vigraman is currently working as associate professor in Dept of Mechanical enginnering at national engineering college, India, PH-9486455085, E-mail: tmvig.yanka@gmail.com*

2 EXPERIMENTAL WORK

Powder metallurgy is the process of blending fine powdered materials, pressing them into a desired shape known as compacting, and then heating the compressed material in a controlled atmosphere to bond the material which is known as sintering. The powder metallurgy process generally consists of four basic steps: powder manufacture, powder blending, compacting, and sintering. Compacting is generally performed at room temperature but in few cases it is carried out at higher temperatures. ,'Fe', 'Mn', 'Si', 'Cu' and 'Ni' metal powders are purchased from SD fine metal powder company, Coimbatore. The average particle size of powders is in the range of 23-45 microns. The cold compactions of powders for various compositions were done by using a cylindrical die having a bored hole dimension of 20 mm diameter and 30 mm height. The experiments are conducted by varying the composition of the alloying elements as shown in Table 1. The process parameters are set at two levels and the values are shown in Table 2.

Table 1 Composition of Fe-Mn-Si -alloys.

Composition in wt.%	Fe	Mn	Si	Ni	Cu
Fe-Mn-Si	64	30	6	-	-
Fe-Mn-Si-Ni	63	30	6	1.0	-
Fe-Mn-Si-Ni-Cu	61.5	30	6	1.0	1.5

Table 2 Experimental parameter setting.

Sample No	Composition	Pressure MPa	Temperature °C
1	Fe-Mn-Si	500	950
2	Fe-Mn-Si-Ni	530	1000
3	Fe-Mn-Si-Ni-Cu	560	1050

Figure 1 (a) Tensile test specimen fixed in a fixture and (b) mounted in tensile testing machine and (c) broken tensile test specimens.

The sintering process for the powder preforms were carried out in the temperature range of 950-1050 ◦ C for 2 hours followed by furnace cooling. The optical microscopic examination of the samples were carried out by polishing them using different grades of silicon carbide abrasive sheets. Finally, the samples were polished with Alumina compound to obtain mirror finish. The polished surfaces are etched with a chemical etchant containing 5 g $Cucl_3$, 15 ml ethanol and 10 ml HNO_3. The mechanical properties of the Fe–Mn–Si cylindrical specimens were evaluated by conducting tensile test and hardness assessment on the rectangular section of 6 mm width and 2 mm thick specimens. The tensile test specimens were of 2 mm in diameter and 15 mm in gauge length. The tensile test is conducted using a specially designed fixture as shown in Figure 1 (a) to hold the specimen and this fixture is held in a tensile testing machine of 200 ton capacity as shown in Figure 1 (b). The load range of the machine is very high, therefore, a load cell having 7000 N capacity is used to measure the tensile load applied on the small test specimens. The broken tensile test specimens are shown in Figure 1 (c). The shape memory properties were evaluated by carrying out bend test on thin strips of rectangular section specimens with the dimensions of 3 mm × 0.5 mm × 30 mm.

3 RESULTS AND DISCUSSION

3.1 Optical microscopy

The optical micrograph shown in Figure 2 (a), (b) and (c), corresponds to the three samples namely sample 1, sample 2 and sample 3 as given in Table 2. The micrographs reveal a combination of fine grains and coarse grains. The micrograph in Figure 2 (a) has nearly 85% ferrite and 15% austenite phase. The brown colour regions in the micrograph are identified as ferrite phase and the regions in green colour are identified as austenite phase. Austenite phase is present because of 30 % Mn addition in this alloy. Manganese has 50% austenite and 50% ferrite stabilizing effect. At the grain boundary triple points segregation of compounds such as secondary phase particles and intermetallic compounds are seen. At few places some spherical dark phases are noted which is identified as secondary phase particles. The secondary phases are FeO_2 and Fe_3C. The thick and dark grain boundaries at few places reveal the precipitation of Mn_3Si compound.

In Figure 2 (b), Fe-Mn-Si-Ni alloy microstructure is shown. Only at few places grain boundaries are seen. Close look at the micrograph reveals the presence of very fine grains in the alloy. The percentage of ferrite and austenite phases are 80% and 20%, respectively. The brown colour regions in the micrographs are identified as ferrite phase and the regions in green colour are identified as austenite phase. Austenite phase is present because of 30 % Mn and 1% Ni addition in this alloy. Manganese has 50% austenite and 50% ferrite stabilizing effect. At few places some spherical dark phases are noted which are identified as secondary phases. The secondary phases are identified as FeO_2

and Fe_3C. Thickening of grain boundaries are not found in this micrograph.

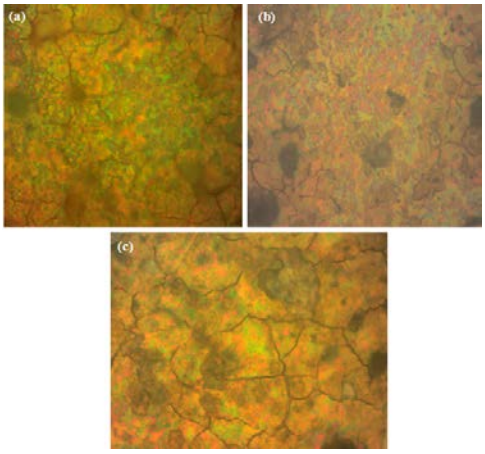

Figure 2 Optical micrographs of the (a) sample 1(b) sample 2 (c) sample 3.

The micrograph shown in Figure 2 (c) reveals the presence of large grains in the microstructure. Grain growth is observed in this alloy combination Fe-Mn-Si-Ni-Cu processed at 1050 ^oC. The sintering temperature is closer to the melting point of copper, therefore, eutectic compound might have formed at few places. Also, the molten copper binds the alloy and improves the mechanical properties. At the top right side of the micrograph few recrystallized grains or region resembling eutectic mixture is seen. The average grain size is less than 25 microns. The microstructure consists of ferrite and austenite phases. The ratio of ferrite and austenite in this alloy is 75:25. This alloy has austenite stabilizing elements such as 'Mn', 'Ni' and 'Cu', therefore the austenite content is more. At few places some spherical dark phases are noted which are identified as secondary phases. The secondary phases are classified as FeO_2 and Fe_3C. Thick grain boundaries are not found in this micrograph.

3.2 TENSILE STRENGTH

The tensile test results of the various samples are shown in Table 3. The sample 1 as mentioned in Table 3 has yielded a tensile strength of 279 MPa. The composition of the alloy is Fe-30%Mn-6%Si and the poor strength exhibited by this alloy is attributed to lower sintering temperature. A maximum tensile strength of 301MPa was observed for the sample 2 as given in Table 2. The maximum tensile strength obtained for this sample is attributed to dispersion of secondary phase particles and intermetallic compounds. Further, fine grains increases strength of the alloy. For the sample 3 containing Fe-30%Mn-6%Si-1Ni-1.5%Cu the tensile strength value obtained is 286 MPa. This tensile strength value is better than the strength value obtained for the sample 1. The increase in strength is attributed to the addition of more amounts of alloying elements and therefore, more amounts of intermetallic compounds are formed because of this dispersion strengthening effect is imparted.

The graphical plot between the sample number and tensile strength of the samples is shown in Figure 3. The sample 2 has exhibited maximum tensile strength compared to all the other samples. The samples 1 and 3 exhibited limited ductility and failed in a brittle manner in comparison with the sample 2.

S. No	*Composition in Wt. %*	*Average tensile strength in MPa*
1	Fe-30Mn-6Si	279
2	Fe-30Mn-6Si-1Ni	301
3	Fe-30Mn-6Si-1Ni-1.5Cu	286

Table 3 Tensile strength of the powder samples.

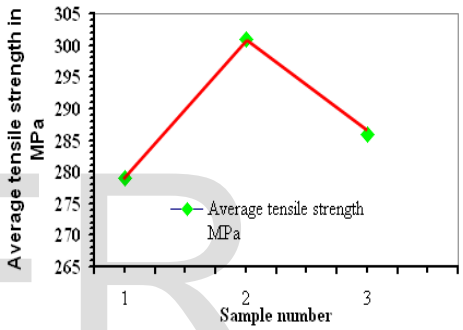

Figure 3 A graphical plot between sample number vs. tensile strength.

3.3 Shape memory effect testing method:

The specimens were bent to 90° using a cylindrical bar at room temperature. Because of this strain subjected to the specimen phase transformation took place. The 'γ' to 'ε' phase transformation was observed in the bent samples. The bent samples were heated in a furnace upto 300 °C during recovery treatment and the recovery angle was measured. The recovery angle measurement method is shown in Figure 4. The measured values of strain and percentage of recovery are recorded in the Table 4.

Figure 4 Shows the SMA strip after recovery.

The strain and shape recovery in percentage of one-way SMA is estimated using the following equations.

$$\varepsilon = \left(\frac{t}{D+t}\right) \times 100\% \ldots\ldots\ldots\ldots\ldots\ldots (1)$$

$$\eta = \left(\frac{90-\theta_1}{\theta_1}\right) \times 100\% \ldots\ldots\ldots\ldots\ldots\ldots (2)$$

Where

η =% of recovery

θ= strip recovery angle in °

ε= strain deformation

t= thickness of strip in mm

D= diameter of roller in mm

Table 4 Shape memory effect of Fe-Mn-Si alloys.

Com-position	Roller diameter Dmm	Thick-ness of strip mm	Strip re-cover-y angle θ°	Strain defor-mation	Per-centag-e of recov-ery
Fe-30Mn-6Si-1Ni	20	0.5	75	20%	16.66
Fe-30Mn-6Si-1Ni-1.5Cu	20	0.5	78	20%	13.33

4 Conclusion

The shape memory alloys Fe-Mn-Si with the addition of 'Cu' and 'Ni' were produced by varying the parameters such as composition, compacting pressure and sintering temperature.These alloys possessed good machinability, moderate 301 MPa was exhibited by a Fe-30%Mn-6%Si-1%Ni alloy. The sample failed in a ductile manner.Brittle fracture was prevalent in the shape memory alloys such as Fe-30%Mn-6%Si and Fe-30%Mn-6%Si-1%Ni-1.5%Cu.The hardness values of the samples were not so high. A maximum hardness of 78 in Rockwell hardness B scale ductility and strength. A maximum tensile strength of was recorded

References

[1] Characteristics and applications of Fe-Mn-Si-based shape memory alloys. waji materia co., ltd.1989.

[2] Chenxu Zhao, Gongyin Liang, Chenglao Li and Zhihao Jin. (1998) 'Influence of cerium, titanium and nitrogen on shape memory effect of Fe-Mn-Si-Cr-Ni alloys' Scripta Materialia, Vol. 38 (7), pp. 1163–1168.

[3] Shipu Chen Jianfeng Wan, Xing Huang, Hsu T Y. (2002) ' Effect of Nitrogen Addition on Shape Memory Characteristics of Fe–Mn–Si–Cr Alloy' Materials Transactions, Vol. 43 (5), pp. 920-925.

[4] Kajiwara Yosaku Ike, Masarou Kojima, Takatoshi Ogawa. (2006) 'Development of Prestressed Concrete Using Fe-Mn-Si-Based Shape Memory Alloys Containing NbC' Materials Transactions, Vol. 47 (3), pp. 580 – 583.

[5] Bobby Kannan M, Singh Ramanb R K, Khoddam S. (2008) 'Comparative studies on the corrosion properties of a Fe–Mn–Al–Si steel and an interstitial-free steel' Corrosion Science, Vol. 50, pp. 2879–2884.

[6] Pricop B, Soyler U, Comneci R I, Ozkal B, Bujoreanua L G. (2010) 'Mechanical cycling effects at Fe-Mn-Si-Cr-Ni SMA's obtained by powder metallurgy' physics procedia, Vol. 10, pp. 125–131

[7] Takeshi Saito, Karolina Gąska, Akito Takasaki, Czesław Kapusta. (2010) 'Fabrication of Fe-Mn-Si alloy by mechanical alloying and direct current sintering' physics procedia, Vol. 30, pp. 62–67.

[8] Nevin Balo S, Yakuphanoglu F. (2013) 'The effects of cr on isothermal oxidation behavior of Fe–30Mn–6Si alloy' Thermochimica Acta, Vol. 560, pp. 43– 46.

[9] Y.Wen, H.Pen, C.Wang, Q.Yu, N.Li, Adv.Eng.Mater.13 (1–2) (2011)48.

[10] Shashi Chillappagari, Hein Trip 'Copper Stress Affects Iron Homeostasis by Destabilizing Iron-Sulfur Cluster Formation in Bacillus subtilis'30, 9751 NN,Haren.